

Optimal performance of a three-level quantum refrigerator

Varinder Singh,^{1,2,*} Tanmoy Pandit,^{1,†} and Ramandeep S. Johal^{1,‡}

¹*Department of Physical Sciences, Indian Institute of Science Education and Research Mohali, Sector 81, S.A.S. Nagar, Manauli PO 140306, Punjab, India*

²*Department of Physics, Koç University, Sarıyer, Istanbul, 34450, Turkey*



(Received 8 October 2019; revised manuscript received 2 May 2020; accepted 26 May 2020; published 15 June 2020)

We study the optimal performance of a three-level quantum refrigerator using two different objective functions: cooling power and χ function. For both cases, we obtain general expressions for the coefficient of performance (COP) and derive its well-known lower and upper bounds for the limiting cases when the ratio of system-bath coupling constants at the hot and cold contacts approaches infinity and zero, respectively. We also show that the cooling power can be maximized with respect to one control frequency, while χ function can be maximized globally with respect to two control frequencies. Additionally, we show that in the low-temperature regime, our model of refrigerator can be mapped to Feynman's ratchet and pawl model, a classical mesoscopic heat engine. In the parameter regime where both cooling power and χ function can be maximized, we compare the cooling power of the quantum refrigerator at maximum χ function with the maximum cooling power.

DOI: [10.1103/PhysRevE.101.062121](https://doi.org/10.1103/PhysRevE.101.062121)

I. INTRODUCTION

In 1824, Carnot discovered that the efficiency of any heat engine operating between two reservoirs at temperatures T_h and T_c ($T_c < T_h$), is bounded from above by the Carnot efficiency, $\eta_C = 1 - T_c/T_h$. If a heat cycle is reversed—turning it into a refrigerator—then the corresponding measure, called the coefficient of performance (COP), is similarly bounded from above by $\epsilon_C = T_c/(T_h - T_c)$. Somehow, the optimization analysis of irreversible refrigerators [1–4] turns out to be more involved than that of heat engines. For instance, power output is a reasonable objective to maximize for a heat engine. Under the assumptions of endoreversibility and Newton's law for heat transfer, the efficiency at maximum power was derived by Curzon-Ahlborn (CA) [5]:

$$\eta_{CA} = 1 - \sqrt{1 - \eta_C}. \quad (1)$$

Then, Esposito and coauthors [6] introduced the concept of a low-dissipation heat engine and obtained lower and upper bounds on the efficiency at maximum power. Further, for the symmetric dissipation at the hot and the cold contacts, they reproduced CA value. Izumida and Okuda [7] introduced minimally nonlinear irreversible model to describe low-dissipation limit within an Onsager-like framework. Further, low-dissipation behavior is also obtained within a linear-irreversible framework using an auxiliary, finite-heat reservoir [8], where CA value is obtained as the lower limit of a class of efficiencies at maximum power for the symmetric case. CA-efficiency is also obtained using inference in models of limited information based on Jeffreys prior probability

function [9,10]. Recently, in a global approach to irreversible entropy generation [11], which is independent of the specific nature of heat cycle, CA-efficiency was related to geometric mean value of the heat exchanged with reservoirs. In contrast to the engines operating at maximum power, some recent studies [12–15] analyzed the performance of irreversible heat engines operating at a given power and found lower and upper bounds on the efficiency of such engines [14,15].

However, for refrigerators, maximizing the rate of refrigeration or the cooling power (CP) seems to be the desirable objective. CP cannot be maximized, however, within endoreversible models with certain heat transfer laws, such as Newton's law [1]. In such cases, maximum CP is obtained for a vanishing COP, which is not a useful result, since real refrigerators operate with finite values of both CP and COP. Similarly, for the low-dissipation refrigerator model, a generic maximum for CP does not exist. However, if the input work is first minimized for a given cycle time, then CP can be maximized, as shown in Ref. [16]. Notably, the maximization of CP has also been studied for low-dissipation absorption refrigerator [17].

Yan and Chen [1] had earlier proposed to maximize a new criterion, $\chi = \epsilon \dot{Q}_c$, which gives equal emphasis to both COP (ϵ) and CP (\dot{Q}_c), and thus analyzes a tradeoff function between these two quantities. For instance, the COP at maximum χ using Newton's law within endoreversible approximation is given by

$$\epsilon_{CA} = \sqrt{1 + \epsilon_C} - 1, \quad (2)$$

which also holds for many models of classical [10,11,16,18–20] and quantum refrigerators [3,21]. Further, Agrawal and Menon [2] showed that CP of endoreversible refrigerators becomes optimizable if we take into account the time spent on adiabatic branches. However, this results in a model-dependent expression for the COP. Similarly, CP of a classical

*varindersingh@iisermohali.ac.in

†tanmoypandit@iisermohali.ac.in

‡rsjohal@iisermohali.ac.in

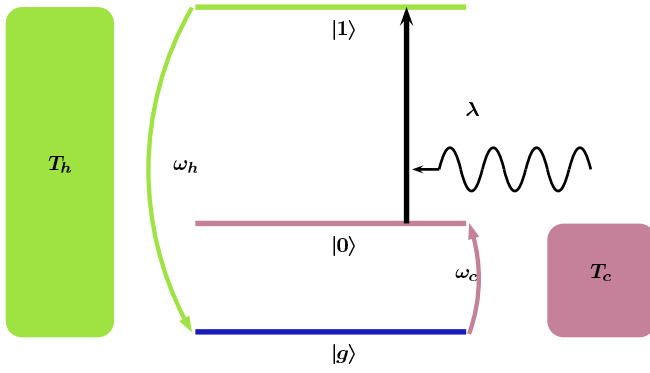


FIG. 1. Schematic of three-level laser refrigerator continuously coupled to two heat reservoirs at temperatures T_c and T_h with coupling constants Γ_c and Γ_h , respectively. A single-mode classical field drives the transition between levels $|0\rangle$ and $|1\rangle$, and λ represents the strength of system-field coupling.

endoreversible refrigerator can be maximized by considering non-Newtonian laws of heat transfer, employed earlier to maximize the power output in CA model [1]. Again, this results in nonuniversal formulas for the COP of the refrigerator that depend on phenomenological heat conductivities. Recently, carrying the research in optimization of refrigerators one step forward, Correa *et al.* maximized the CP of a quantum endoreversible refrigerator in high-temperature regime and obtained model-independent expression for the COP [22].

In this work, we study the optimal performance of a three-level quantum refrigerator [23,24]. It is regarded that the study of three-level systems pioneered by Scovil and Schulz-DuBois (SSD), started the field of quantum thermodynamics [25–31]. In recent years, these systems have also been employed to study quantum heat engines (refrigerators) [32–38] and quantum absorption refrigerators [39–47]. Our choice of the model is motivated by the observation that it can be maximized for both CP and χ function and yields model-independent expressions for lower and upper bounds on the COP in each case, i.e., ones that are free of the specific parameters of the model.

The paper is organized as follows. In Sec. II, we discuss the model of SSD refrigerator. In Sec. III, we maximize the CP of the refrigerator and obtain the general expression for the optimal COP, and find lower and upper bounds on the COP. In Sec. IV, we maximize the χ function and obtain analytic expressions for the COP for two-parameter as well as one-parameter optimization scheme. We conclude in Sec. V.

II. MODEL OF THREE-LEVEL QUANTUM REFRIGERATOR

The model consists of a three-level atomic system continuously coupled to two thermal reservoirs and to a single mode of classical electromagnetic field as shown in Fig. 1. In refrigerators, heat is extracted from the cold reservoir and dumped into the hot reservoir, with the help of an external agent. The power input mechanism is modeled by an external single mode field coupled to the levels $|0\rangle$ and $|1\rangle$, inducing transitions between these levels. The population in level $|1\rangle$ then relaxes to level $|g\rangle$ by rejecting heat to the hot bath. The

system then jumps from level $|g\rangle$ to level $|1\rangle$ by absorbing energy from the cold bath. The Hamiltonian of the system is given by: $H_0 = \hbar \sum_k \omega_k |k\rangle \langle k|$, where the summation runs over all three states and ω_k represent the relevant atomic frequencies. The interaction with the single mode lasing field of frequency ω , under the rotating wave approximation (RWA), is described by the semiclassical hamiltonian: $V(t) = \hbar \lambda (e^{i\omega t} |1\rangle \langle 0| + e^{-i\omega t} |0\rangle \langle 1|)$, where λ is the field-atom coupling constant. Note that, RWA is valid under conditions of near-resonance and a weak system-bath coupling.

The most general time-independent dissipator generating a completely positive, trace-preserving and linear evolution was derived by Gorini, Kossakowski, and Sudarshan [48], and Lindblad [49]. The time evolution of the system is described by the following master equation:

$$\dot{\rho} = -\frac{i}{\hbar} [H_0 + V(t), \rho] + \mathcal{L}_h[\rho] + \mathcal{L}_c[\rho], \quad (3)$$

where $\mathcal{L}_{h(c)}[\rho]$ represents the dissipative Lindblad superoperator describing the system-bath interaction with the hot (cold) reservoir:

$$\begin{aligned} \mathcal{L}_h[\rho] = & \Gamma_h (n_h + 1) (2|g\rangle \langle g| \rho_{11} - |1\rangle \langle 1| \rho - \rho |1\rangle \langle 1|) \\ & + \Gamma_h n_h (2|1\rangle \langle 1| \rho_{gg} - |g\rangle \langle g| \rho - \rho |g\rangle \langle g|), \end{aligned} \quad (4)$$

$$\begin{aligned} \mathcal{L}_c[\rho] = & \Gamma_c (n_c + 1) (2|g\rangle \langle g| \rho_{00} - |0\rangle \langle 0| \rho - \rho |0\rangle \langle 0|) \\ & + \Gamma_c n_c (2|0\rangle \langle 0| \rho_{gg} - |g\rangle \langle g| \rho - \rho |g\rangle \langle g|). \end{aligned} \quad (5)$$

Here Γ_h and Γ_c are the Weisskopf-Wigner decay constants, and $n_{h(c)} = 1/(\exp[\hbar\omega_{h(c)}/k_B T_{h(c)}] - 1)$ is the average occupation number of photons in hot (cold) reservoir satisfying the relations, with $\omega_c = \omega_0 - \omega_g$, $\omega_h = \omega_1 - \omega_g$.

For our model, it is possible to find a rotating frame in which the steady-state density matrix ρ_R is time independent [10]. Defining $\bar{H} = \hbar(\omega_g |g\rangle \langle g| + \frac{\omega}{2} |1\rangle \langle 1| - \frac{\omega}{2} |0\rangle \langle 0|)$, an arbitrary operator A in the rotating frame is given by $A_R = e^{i\bar{H}t/\hbar} A e^{-i\bar{H}t/\hbar}$. It can be seen that $\mathcal{L}_h[\rho]$ and $\mathcal{L}_c[\rho]$ remain unchanged under this transformation. The time evolution of the system density matrix in the rotating frame can be written as

$$\dot{\rho}_R = -\frac{i}{\hbar} [H_0 - \bar{H} + V_R, \rho_R] + \mathcal{L}_h[\rho_R] + \mathcal{L}_c[\rho_R], \quad (6)$$

where $V_R = \hbar \lambda (|1\rangle \langle 0| + |0\rangle \langle 1|)$.

In a series of papers [50–52], Boukobza and Tannor formulated a new way of quantifying heat and work for weak system-bath coupling [53]. Then, the input power and heat flux of the refrigerator are defined as follows:

$$P = \frac{i}{\hbar} \text{Tr}([H_0, V_R] \rho_R), \quad (7)$$

$$\dot{Q}_c = \text{Tr}(\mathcal{L}_c[\rho_R] H_0). \quad (8)$$

Calculating the traces (see Appendix A) appearing in the right hand side of Eqs. (7) and (8), the power input and heat flux can be written as

$$P = i\hbar \lambda (\omega_h - \omega_c) (\rho_{01} - \rho_{10}), \quad (9)$$

$$\dot{Q}_c = i\hbar \lambda \omega_c (\rho_{01} - \rho_{10}), \quad (10)$$

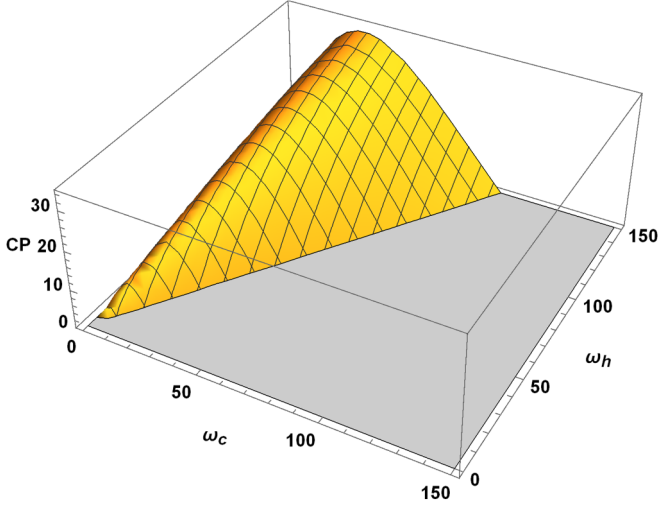


FIG. 2. 3D plot of CP [Eq. (A11)] in terms of control frequencies ω_c and ω_h for $\hbar = 1$, $k_B = 1$, $\Gamma_h = 3.4$, $\Gamma_c = 3.2$, $\lambda = 3$, $T_h = 60$, $T_c = 40$.

where $\rho_{01} = \langle 0|\rho_R|1\rangle$ and $\rho_{10} = \langle 1|\rho_R|0\rangle$. Note that the input power and cooling flux above are independent of coordinate transformations. For a given configuration of the system with $\omega_h > \omega_c$, we use the convention $P > 0$ and $\dot{Q}_c > 0$ to signify the operation as a refrigerator, that regards energy fluxes entering into the three-level atom as positive. Further, $P > 0$ implies that the electric field is being attenuated in case of the refrigerator, in contrast to the case of a heat engine where it is amplified [52]. From Eq. (A11), this requires $n_c > n_h$, which is related to the fact that $\rho_{11} - \rho_{00} < 0$. This implies that there is no population inversion between excited levels in the operation of a refrigerator.

Finally, from $n_c > n_h$, we derive the condition: $\omega_c/T_c < \omega_h/T_h$. This leads to the conclusion that the COP as given by

$$\epsilon = \frac{\dot{Q}_c}{P} = \frac{\omega_c}{\omega_h - \omega_c} \leq \epsilon_C \quad (11)$$

is bounded from above by the Carnot value.

III. MAXIMIZATION OF COOLING POWER

In this section, we maximize CP of the quantum refrigerator and solve for the corresponding COP. The general expression for CP is derived in Appendix A, see Eq. (A11). We show the 3D plot of CP with respect to ω_c and ω_h in Fig. 2. It is clear from the figure that a well defined maximum with respect to ω_c exists whereas there is no such maximum with respect to ω_h . In other words, CP is optimizable with respect to ω_c only. We have played with a wide range of different values of the concerned parameters ($\Gamma_{c,h}$, $T_{c,h}$, λ), but the basic trend of the graph remains the same and it does not change the main result.

However, in this case, an analytic expression for the COP seems hard to obtain. This necessitates the following remark. Although, the above framework of Sec. II assumes both the system-field coupling as well as the system-bath coupling to be weak, however, the analytic results to derived below are

valid in the limit when the former is assumed large compared to the latter ($\lambda \gg \Gamma_{c,h}$) [35].

Thus, to derive the COP in a closed form, we work in the high-temperature regime [41,54–57] and assume that the system-field coupling to be strong compared to the system-bath coupling. In this regime, it is possible to obtain model-independent performance benchmarks for both quantum engines and refrigerators [22,55,56,58]. Then, we can approximate $n_h \simeq k_B T_h / \hbar \omega_h$ and $n_c \simeq k_B T_c / \hbar \omega_c$, which simplifies the expression for CP to the form

$$\dot{Q}_c = 2\hbar\Gamma_h \frac{\omega_c(\tau\omega_h - \omega_c)}{3(\tau\omega_h + \gamma\omega_c)}, \quad (12)$$

where $\gamma = \Gamma_h/\Gamma_c$ and $\tau = T_c/T_h \equiv \epsilon_C/(1 + \epsilon_C)$. One can argue that a unique maximum of \dot{Q}_c with respect to both ω_h and ω_c cannot exist. For, if we assume the values of the reservoir temperatures and coupling constants to be fixed, then under the scaling $(\omega_h, \omega_c) \rightarrow (\alpha\omega_h, \alpha\omega_c)$, where α is a certain positive number, the CP also scales as $\dot{Q}_c \rightarrow \alpha\dot{Q}_c$. Thus, there cannot exist a unique optimal configuration $(\hat{\omega}_h, \hat{\omega}_c)$ that yields a unique maximum for CP.

However, for a given value of ω_h , $\dot{Q}_c \rightarrow 0$ for both $\omega_c \rightarrow 0$ and $\omega_c \rightarrow \tau\omega_h$. In between these limiting values of ω_c , \dot{Q}_c exhibits a maximum. Thus, setting $\partial\dot{Q}_c/\partial\omega_c = 0$, we obtain the optimal solution,

$$\omega_c^* = \omega_h \frac{(\sqrt{1+\gamma} - 1)\tau}{\gamma}, \quad (13)$$

with the COP at maximum CP as given by

$$\epsilon^* = \frac{\epsilon_C}{1 + \sqrt{1 + \gamma}(1 + \epsilon_C)}. \quad (14)$$

We note that ϵ^* is a monotonically decreasing function of γ . Thus, we can obtain lower (upper) bound on the COP at maximum CP by letting $\gamma \rightarrow \infty$ ($\gamma \rightarrow 0$):

$$0 \leq \epsilon^* \leq \frac{\epsilon_C}{2 + \epsilon_C}. \quad (15)$$

Note that the limits of γ values should be achieved while maintaining $\Gamma_h \ll \omega_h$ and $\Gamma_c \ll \omega_c$, to ensure the weak-dissipation regime.

The above bounds can be obtained in a variety of other models [4,59] and approaches [11,16]. In particular, the upper bound above is also obtained for an endoreversible quantum refrigerator (see Eq. (14) in Ref. [22] for $d_c = 1$) operating at maximum CP. The reason behind this is that like Ref. [22], we also consider here the unstructured bosonic baths with a flat spectral density in one-dimension ($d_c = 1$).

Similarly, substituting Eq. (13) in Eq. (12) the optimal CP is given by

$$\dot{Q}_c^* = 2\hbar\Gamma_h\omega_h \frac{(2 + \gamma - 2\sqrt{1+\gamma})\epsilon_C}{3(1 + \epsilon_C)\gamma^2}. \quad (16)$$

For future reference, we find the expressions for \dot{Q}_c^* in the limiting cases $\gamma \rightarrow 0$ and $\gamma \rightarrow \infty$:

$$\dot{Q}_c^*(\gamma \rightarrow 0) = \frac{\hbar\Gamma_h\omega_h}{2} \frac{\epsilon_C}{3(1 + \epsilon_C)}, \quad (17)$$

$$\dot{Q}_c^*(\gamma \rightarrow \infty) = 2\hbar\Gamma_c\omega_h \frac{\epsilon_C}{3(1 + \epsilon_C)}. \quad (18)$$

TABLE I. COP at global optimization of χ function. Here $T_c = 50$, $T_h = 100$. The results shown in first, second, and third rows correspond to $\Gamma_h = 1$, $\Gamma_c = 2000$; $\Gamma_h = 1$, $\Gamma_c = 1$; and $\Gamma_h = 2000$, $\Gamma_c = 1$, respectively. For the given values of T_c and T_h , $\epsilon_{CA} = 0.414213$.

	$\lambda = 1$	$\lambda = 100$	$\lambda = 10000$
$\gamma = 0.0005$	$\epsilon = 0.459333$	$\epsilon = 0.475244$	$\epsilon = 0.476904$
$\gamma = 1$	$\epsilon = 0.441015$	$\epsilon = 0.43729$	$\epsilon = 0.437283$
$\gamma = 2000$	$\epsilon = 0.42461$	$\epsilon = 0.372163$	$\epsilon = 0.346034$

As mentioned above, for a given value of ω_c , \dot{Q}_c [Eq. (12)] does not exhibit a maximum with respect to ω_h in its allowed range $\omega_c/\tau < \omega_h < \infty$ (see also Table II).

IV. OPTIMIZATION OF χ FUNCTION

The χ function, $\chi = \epsilon \dot{Q}_c$ has already been shown to be a suitable figure of merit in the study of optimal performance of classical [18,19] as well as quantum refrigerators [3,21,60]. In the following, we reaffirm this observation by pointing out that in the case of SSD refrigerator, it is possible to maximize the χ function with respect to control frequencies ω_c and ω_h . This presents the advantage of optimizing χ function over CP which can only be maximized with respect to a single parameter.

A. Global optimization

In the general case, again it is not possible to obtain analytic expression for the COP. Therefore, we maximize Eq. (A12) numerically and present our results in Table I.

1. Low-temperature regime

The low-temperature regime is governed by the condition: $k_B T_{c,h} \ll \hbar \omega_{c,h}$, such that $n_{c,h} \approx e^{-\hbar \omega_{c,h}/k_B T_{c,h}} \ll 1$. Simplifying Eq. (A12), we get the expression for χ function as follows:

$$\chi = \frac{2\hbar\lambda^2\Gamma_c\Gamma_h(n_c - n_h)\omega_c^2}{(\Gamma_c + \Gamma_h)(\lambda^2 + \Gamma_c\Gamma_h)(\omega_h - \omega_c)}. \quad (19)$$

Maximization of Eq. (19), with respect to ω_h and ω_c , yields the following equations:

$$e^{\hbar\omega_h/k_B T_h - \hbar\omega_c/k_B T_c} = 1 + \frac{\hbar\omega_c\epsilon_C}{k_B T_c(1 + \epsilon_C)}, \quad (20)$$

$$e^{\hbar\omega_h/k_B T_h - \hbar\omega_c/k_B T_c} = \frac{k_B T_c(2 + \epsilon)}{k_B T_c(2 + \epsilon) - \hbar\omega_c}. \quad (21)$$

The above equations cannot be solved analytically for ω_h and ω_c . However, they can be combined to give the following transcendental equation (see Appendix B):

$$\exp\left[\frac{(2\epsilon_C - \epsilon)(\epsilon_C - \epsilon)}{\epsilon(1 + \epsilon_C)\epsilon_C}\right] = \frac{(2 + \epsilon)\epsilon_C}{\epsilon(1 + \epsilon_C)}, \quad (22)$$

which clearly indicates that COP at maximum χ function depends upon ϵ_C only and is independent of system parameters. Equation (22) along with the expression, $\epsilon_{CA} = \sqrt{1 + \epsilon_C} - 1$, is plotted in Fig. 3, from which it is clear that COP of the SSD

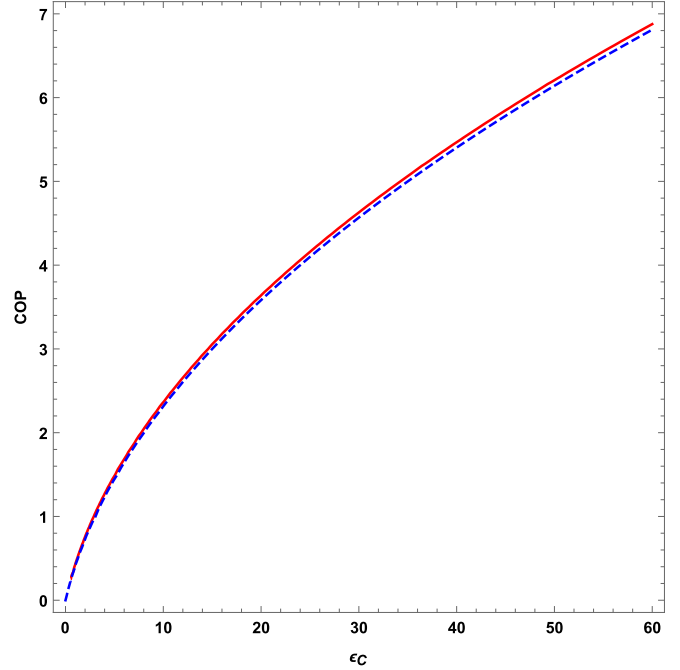


FIG. 3. Plot of the COP versus ϵ_C . Solid red curve represents Eq. (22) and dashed blue curve represents the equation $\epsilon_{CA} = \sqrt{1 + \epsilon_C} - 1$.

refrigerator operating in low-temperature regime is higher than, though quite close to ϵ_{CA} . See also Appendix E for the mapping of the refrigerator model in the above regime to Feynman's ratchet and pawl model.

B. One parameter optimization in high-temperature regime

High temperatures along with a strong system-field coupling ($\lambda \gg \Gamma_{c,h}$) is another operational regime in which we can obtain model-independent benchmarks from the optimization of χ function. In this regime, the expression for χ is simplified to

$$\chi = \epsilon \dot{Q}_c = \frac{2\hbar\Gamma_h\omega_c^2(\tau\omega_h - \omega_c)}{3(\tau\omega_h + \gamma\omega_c)(\omega_h - \omega_c)}. \quad (23)$$

A two-parameter maximization by setting $\partial\chi/\partial\omega_c = 0$ and $\partial\chi/\partial\omega_h = 0$, does not give a nontrivial solution, which may be understood, using a scaling argument, as we discussed for CP in Sec. III. In view of this, we maximize χ function alternately with respect to ω_h (ω_c fixed) and ω_c (ω_h fixed). As shown in Table II, a maximum for χ is expected to exist under both of these situations. For a fixed ω_c , setting $\partial\chi/\partial\omega_h = 0$, we obtain

$$\omega_h = \omega_c \frac{\gamma - \tau(1 + \gamma)}{\tau[1 - \sqrt{(1 + \gamma)(1 - \tau)}]}. \quad (24)$$

Substituting in Eq. (11), and writing in terms of Carnot COP ϵ_C , we get the following form of COP at maximum χ function:

$$\epsilon^* = \frac{\epsilon_C}{1 + \sqrt{(1 + \gamma)(1 + \epsilon_C)}}. \quad (25)$$

Again ϵ^* is monotonic decreasing function of γ . Therefore, we can obtain lower and upper bounds on the COP by putting

TABLE II. Limiting behavior of CP, COP and the χ function when one frequency, either ω_h or ω_c , is kept fixed. The maximum of CP exists only when ω_h is kept fixed, while the maximum of χ function is possible in both scenarios.

Fixed	Variable	CP (\dot{Q}_c)	COP (ϵ)	$\chi = \epsilon \dot{Q}_c$
ω_h	$\omega_c \rightarrow 0$	$\dot{Q}_c \rightarrow 0$	$\epsilon \rightarrow 0$	$\chi \rightarrow 0$
	$\omega_c \rightarrow \tau \omega_h$	$\dot{Q}_c \rightarrow 0$	$\epsilon \rightarrow \epsilon_C$	$\chi \rightarrow 0$
ω_c	$\omega_h \rightarrow \omega_c/\tau$	$\dot{Q}_c \rightarrow 0$	$\epsilon \rightarrow \epsilon_C$	$\chi \rightarrow 0$
	$\omega_h \rightarrow \infty$	$\dot{Q}_c \rightarrow 2\hbar\Gamma_h\omega_c$	$\epsilon \rightarrow 0$	$\chi \rightarrow 0$

$\gamma \rightarrow \infty$ and $\gamma \rightarrow 0$, respectively (see Fig. 4):

$$\epsilon_- \equiv 0 \leq \epsilon^* \leq \epsilon_{CA}. \quad (26)$$

The lower bound, $\epsilon_- = 0$, concurs with the lower bound of low-dissipation [61] and minimally nonlinear irreversible models of refrigerators [19]. As mentioned earlier, the upper bound, ϵ_{CA} , was first derived for a classical endoreversible refrigerator [1]. Under the conditions of tight-coupling and symmetric dissipation, ϵ_{CA} can also be obtained for the low-dissipation [18] and minimally nonlinear irreversible refrigerators [19]. For a quantum Otto refrigerator, the COP emerges to be equal to ϵ_{CA} in the classical limit (high-temperature limit) [21].

Next, we maximize χ with respect to ω_c while keeping ω_h constant. In this case, $\partial\chi/\partial\omega_c = 0$ yields the following equation:

$$\frac{\omega_c[\gamma\omega_c^3 + 2\omega_h(\tau - \gamma)\omega_c^2 - \tau\omega_h^2(3 + \tau - \gamma)\omega_c + 2\tau^2\omega_h^3]}{(\omega_c - \omega_h)^2(\gamma\omega_c + \tau\omega_h)} = 0. \quad (27)$$

Due to *casus irreducibilis* (see Appendix D), the roots of the cubic equation inside the square brackets above can only be expressed using complex radicals, although the roots are actually real. We can still obtain the lower and upper bounds on the COP by solving Eq. (27) for the limiting cases $\gamma \rightarrow \infty$ and $\gamma \rightarrow 0$, respectively. An alternative method is explained

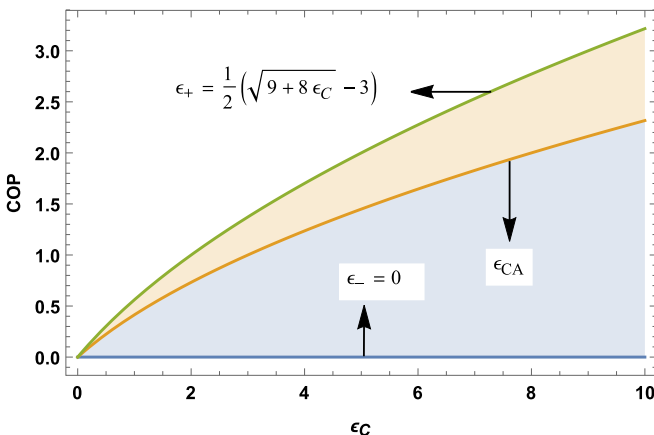


FIG. 4. Plot of the COP at optimal χ versus ϵ_C . ϵ_{CA} divides the parametric region of the COP into two parts. For the optimization of χ function over ω_h , it serves as an upper bound, whereas it is the lower bound on COP for the optimization over ω_c .

in Appendix C that obtains the same expressions. For $\gamma \rightarrow \infty$, the COP is evaluated at CA value. For $\gamma \rightarrow 0$, we obtain the upper bound on the COP as $\epsilon_+ = (\sqrt{9 + 8\epsilon_C} - 3)/2$. Further, although we cannot see analytically, numerical evidence shows that COP lies in the range (see Fig. 4)

$$\epsilon_{CA} \leq \epsilon^* \leq \frac{1}{2}(\sqrt{9 + 8\epsilon_C} - 3) \equiv \epsilon_+. \quad (28)$$

Interestingly, ϵ_{CA} also appears as the lower bound for the optimization of a quantum model of refrigerator consisting of two n -level systems interacting via a pulsed external field [3]. However, the result reported in Ref. [3] was obtained in the linear response regime where $T_c \approx T_h$. In the same model, imposing the condition of equidistant spectra, ϵ_{CA} can be obtained as an upper bound in the classical regime for $n \rightarrow \infty$. The upper bound $\epsilon_+ = (\sqrt{9 + 8\epsilon_C} - 3)/2$ obtained here also serves as the upper limit on the COP for low-dissipation [61] and minimally nonlinear irreversible models [19]. Further, for a two-level quantum system working as a refrigerator, the same upper bound can be derived in the high-temperature regime [60].

V. COOLING POWER AT OPTIMAL χ FUNCTION VERSUS OPTIMAL COOLING POWER

In this section, we compare the CP obtained at maximum χ function with the optimal CP. As CP can be maximized with respect to ω_c only, we can make the comparison only for this case. Dividing Eq. (C5) by Eq. (17), we get the ratio of CP at maximum χ function to the optimal CP, for the limiting case $\gamma \rightarrow 0$:

$$R_{\gamma \rightarrow 0} = \frac{(3 + 2\epsilon_C)\sqrt{9 + 8\epsilon_C} - 9 - 10\epsilon_C}{2\epsilon_C^2}, \quad (29)$$

which approaches the value 8/9 for small ϵ_C , while it vanishes for large ϵ_C (small temperature differences).

Similarly, we get the corresponding ratio for $\gamma \rightarrow \infty$ upon dividing Eq. (C7) by Eq. (18):

$$R_{\gamma \rightarrow \infty} = \frac{\sqrt{1 + \epsilon_C} - 1}{\epsilon_C}, \quad (30)$$

which approaches the value 1/2 for small ϵ_C , while it vanishes for large ϵ_C . We have plotted Eqs. (29) and (30) in Fig. 5, from which it is clear that the ratio is greater for the case $\gamma \rightarrow 0$. Further, it is interesting to note that although both $R_{\gamma \rightarrow 0}$ and $R_{\gamma \rightarrow \infty}$ vanish for $\epsilon_C \rightarrow \infty$, their ratio $R_{\gamma \rightarrow 0}/R_{\gamma \rightarrow \infty} \rightarrow 2\sqrt{2}$ for small temperature differences.

VI. CONCLUSIONS

In this work, we have studied the optimal performance of a three-level atomic system working as a refrigerator. We have studied two different target functions: CP and χ function. Although, in many classical and quantum models of the refrigerator, CP is not a good figure of merit to optimize, in our model, it is a well-behaved function and we have obtained analytic expressions for lower and upper bounds on the COP already derived in some models of classical and quantum refrigerators. However, we notice that CP is maximized only with respect to the control frequency ω_c . In contrast to the

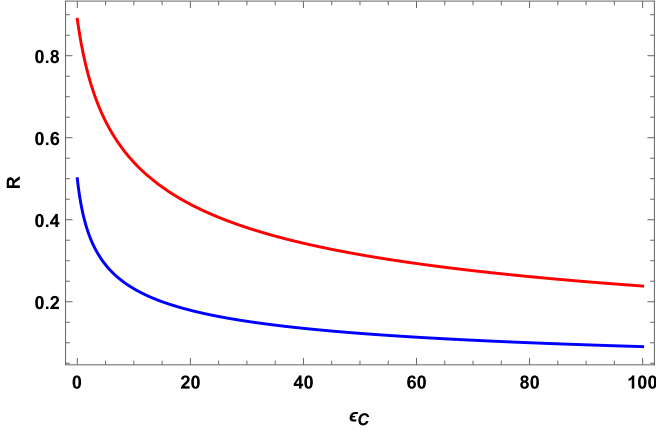


FIG. 5. Ratio (R) of the CP at optimal χ function to the optimal CP. Red and blue curves represent Eqs. (29) and (30), respectively, which approach the value $8/9$ and $1/2$ respectively for $\epsilon_c \rightarrow 0$, and vanish for $\epsilon_c \rightarrow \infty$.

behavior of CP, χ function shows global maximum which makes it a more suitable figure of merit to study the optimal performance of refrigerators. In the general unconstrained regime, we have presented results of numerical optimization in Table I. Then in the low-temperature regime, we showed that the COP of our model is independent of system-bath coupling ($\Gamma_{c,h}$) or system-field coupling (λ), and depends on Carnot COP only, which is a remarkable result. Further, in the high-temperature and strong-coupling regime ($\lambda \gg \Gamma_{c,h}$), we have alternatively performed maximization of χ function with respect to ω_h (ω_c fixed) and ω_c (ω_h fixed). In both cases, we were able to obtain the lower and upper limits on the COP, already well known in the literature on optimization of refrigerators. The possibility of simultaneous maximization of

CP and χ function, enables a comparison between optimal CP in the quantum refrigerator with the CP at optimal χ function, and we conclude that a large system-bath coupling at the cold end (compared to the hot end) yields a higher relative value of CP (see Fig. 5). There are a few classical models [4,19,59] in which both CP and χ function are maximizable. To the best of our knowledge, the present model provides an instance of a quantum thermal machine allowing the same feature. This will aid future studies [62] which explore models in which the performance of quantum machines can be bettered over their classical counterparts.

ACKNOWLEDGMENT

The authors gratefully acknowledge useful discussions with Sibashish Ghosh.

APPENDIX A: STEADY-STATE SOLUTION OF DENSITY MATRIX EQUATIONS

Here, we solve the equations for density matrix in the steady state. Substituting the expressions for H_0 , \bar{H} , V_0 , and using Eqs. (4) and (5) in Eq. (6), the time evolution of the elements of the density matrix are given by following equations:

$$\dot{\rho}_{11} = i\lambda(\rho_{10} - \rho_{01}) - 2\Gamma_h[(n_h + 1)\rho_{11} - n_h\rho_{gg}], \quad (\text{A1})$$

$$\dot{\rho}_{00} = -i\lambda(\rho_{10} - \rho_{01}) - 2\Gamma_c[(n_c + 1)\rho_{00} - n_c\rho_{gg}], \quad (\text{A2})$$

$$\dot{\rho}_{10} = -[\Gamma_h(n_h + 1) + \Gamma_c(n_c + 1)]\rho_{10} + i\lambda(\rho_{11} - \rho_{00}), \quad (\text{A3})$$

$$\rho_{11} = 1 - \rho_{00} - \rho_{gg}, \quad (\text{A4})$$

$$\dot{\rho}_{01} = \dot{\rho}_{10}^*. \quad (\text{A5})$$

Solving Eqs. (A1)–(A5) in the steady state by setting $\dot{\rho}_{mn} = 0$ ($m, n = 0, 1$), we obtain

$$\rho_{10} = \frac{i\lambda(n_h - n_c)\Gamma_c\Gamma_h}{\lambda^2[(1 + 3n_h)\Gamma_h + (1 + 3n_c)\Gamma_c] + \Gamma_c\Gamma_h[1 + 2n_h + n_c(2 + 3n_h)][(1 + n_c)\Gamma_c + (1 + n_h)\Gamma_h]} \quad (\text{A6})$$

and

$$\rho_{01} = \rho_{10}^*. \quad (\text{A7})$$

Calculating the trace in Eq. (7), the input power is given by

$$P = i\hbar\lambda(\omega_h - \omega_c)(\rho_{01} - \rho_{10}). \quad (\text{A8})$$

Similarly evaluating the trace in Eq. (8), heat flux \dot{Q}_c can be written as

$$\dot{Q}_c = \hbar\omega_c(2\Gamma_c[n_c\rho_{gg} - (n_c + 1)\rho_{00}]). \quad (\text{A9})$$

Using the steady-state condition $\dot{\rho}_{00} = 0$ [see Eq. (A2)], Eq. (A9) becomes

$$\dot{Q}_c = i\hbar\lambda\omega_c(\rho_{01} - \rho_{10}). \quad (\text{A10})$$

Substituting Eqs. (A6) and (A7) in Eq. (A10), we have

$$\dot{Q}_c = \frac{2\hbar\lambda^2\Gamma_c\Gamma_h(n_c - n_h)\omega_c}{\lambda^2[(1 + 3n_h)\Gamma_h + (1 + 3n_c)\Gamma_c] + \Gamma_c\Gamma_h[1 + 2n_h + n_c(2 + 3n_h)][(1 + n_c)\Gamma_c + (1 + n_h)\Gamma_h]}. \quad (\text{A11})$$

The expression for χ function, $\chi = \epsilon\dot{Q}_c$, is given by

$$\chi = \frac{2\hbar\lambda^2\Gamma_c\Gamma_h(n_c - n_h)\omega_c^2}{\lambda^2(\omega_h - \omega_c)[(1 + 3n_h)\Gamma_h + (1 + 3n_c)\Gamma_c] + \Gamma_c\Gamma_h[1 + 2n_h + n_c(2 + 3n_h)][(1 + n_c)\Gamma_c + (1 + n_h)\Gamma_h]}. \quad (\text{A12})$$

APPENDIX B: DERIVATION OF EQ. (22)

Optimization of Eq. (19) with respect to ω_h ($\partial\chi/\partial\omega_h = 0$) yields the following condition:

$$\frac{\hbar(\omega_h - \omega_c)}{k_B T_h} e^{-\hbar\omega_h/k_B T_h} - (e^{-\hbar\omega_c/k_B T_c} - e^{-\hbar\omega_h/k_B T_h}) = 0, \quad (\text{B1})$$

which can be simplified to yield

$$e^{\hbar\omega_h/k_B T_h - \hbar\omega_c/k_B T_c} = 1 + \frac{\hbar(\omega_h - \omega_c)}{k_B T_h}. \quad (\text{B2})$$

Using $\epsilon = \omega_c/(\omega_h - \omega_c)$ and $\epsilon_C = T_c/(T_h - T_c)$, Eq. (B2) can be written as

$$e^{\hbar\omega_h/k_B T_h - \hbar\omega_c/k_B T_c} = 1 + \frac{\hbar\omega_c \epsilon_C}{k_B T_c (1 + \epsilon_C) \epsilon}. \quad (\text{B3})$$

Performing similar steps as above, for the optimization of Eq. (19) with respect to ω_c , we obtain

$$e^{\hbar\omega_h/k_B T_h - \hbar\omega_c/k_B T_c} = 1 + \frac{\hbar\omega_c}{k_B T_c (2 + \epsilon) - \hbar\omega_c}. \quad (\text{B4})$$

Comparing Eqs. (B3) and (B4), we obtain the following relation:

$$\frac{\hbar\omega_c}{k_B T_c} = 2 + \epsilon - \frac{\epsilon(1 + \epsilon_C)}{\epsilon_C}. \quad (\text{B5})$$

Then, we can express the exponent in the left hand side of Eq. (B3) as follows:

$$\begin{aligned} \frac{\hbar\omega_h}{k_B T_h} - \frac{\hbar\omega_c}{k_B T_c} &= \frac{\hbar\omega_c}{k_B T_c} \left[\frac{\epsilon_C(1 + \epsilon)}{\epsilon(1 + \epsilon_C)} - 1 \right] \\ &= \frac{(2\epsilon_C - \epsilon)(\epsilon_C - \epsilon)}{\epsilon(1 + \epsilon_C)\epsilon_C}. \end{aligned} \quad (\text{B6})$$

Substituting from Eqs. (B5) and (B6) into (B3), we arrive at Eq. (22).

APPENDIX C: OPTIMIZATION OF χ FUNCTION WITH RESPECT TO ω_c IN HIGH-TEMPERATURE AND STRONG-COUPPLING REGIME

The expression for the χ function is given by

$$\chi = \frac{2\hbar\Gamma_h\omega_c^2(\tau\omega_h - \omega_c)}{3(\tau\omega_h + \gamma\omega_c)(\omega_h - \omega_c)}. \quad (\text{C1})$$

As explained in the Sec. IV, we cannot maximize the above function with respect to ω_c to obtain the roots in real radicals because of the *casus irreducibilis* (see Appendix D). However, we can obtain the real solutions for the limiting cases $\gamma \rightarrow 0$ and $\gamma \rightarrow \infty$. For $\gamma \rightarrow 0$, χ function can be written as

$$\chi = \frac{2\hbar\Gamma_h\omega_c^2(\tau\omega_h - \omega_c)}{3\tau\omega_h(\omega_h - \omega_c)}, \quad (\text{C2})$$

which can be maximized with respect to ω_c for a fixed ω_h to give

$$\omega_c = \frac{\omega_h}{4} (3 + \tau - \sqrt{9 - 10\tau + \tau^2}). \quad (\text{C3})$$

Substituting Eq. (C3) in Eq. (C2) and in the equation $\dot{Q}_c = 2\hbar\Gamma_h\omega_c(\tau\omega_h - \omega_c)/\tau\omega_h$, we get following expressions for the optimal χ function and CP at optimal χ function, respectively:

$$\chi_{\gamma \rightarrow 0}^{*(\omega_h)} = \hbar\Gamma_h\omega_h \frac{27 + 36\epsilon_C + 8\epsilon_C^2 - (9 + 8\epsilon_C)^{3/2}}{12\epsilon_C(1 + \epsilon_C)}, \quad (\text{C4})$$

$$\dot{Q}_{c\gamma \rightarrow 0}^{\chi(\omega_h)} = \hbar\Gamma_h\omega_h \frac{(3 + 2\epsilon_C)\sqrt{9 + 8\epsilon_C} - 9 - 10\epsilon_C}{12\epsilon_C(1 + \epsilon_C)}. \quad (\text{C5})$$

Similarly, for $\gamma \rightarrow \infty$, maximization of χ function, $\chi = 2\hbar\Gamma_c(\tau\omega_h - \omega_c)/(\omega_h - \omega_c)$, yields the following expressions:

$$\chi_{\gamma \rightarrow \infty}^{*(\omega_h)} = \frac{2\hbar\Gamma_c\omega_h(2 + \epsilon_C - \sqrt{1 + \epsilon_C})}{1 + \epsilon_C}, \quad (\text{C6})$$

$$\dot{Q}_{c\gamma \rightarrow \infty}^{\chi(\omega_h)} = \frac{2\hbar\Gamma_c\omega_h(\sqrt{1 + \epsilon_C} - 1)}{1 + \epsilon_C}. \quad (\text{C7})$$

APPENDIX D: CASUS IRREDUCIBILIS

In algebra, *casus irreducibilis* arises while solving a cubic equation. The formal statement of the *casus irreducibilis* is that if a cubic polynomial is irreducible with rational coefficients and has three real roots, then the roots of the cubic equation are not expressible using real radicals and thus, one must introduce expressions with complex radicals, even though the resulting expressions are actually real-valued. It was proven by Wantzel in 1843 [63]. Using the discriminant D of the irreducible cubic equation, one can decide whether the given equation is in *casus irreducibilis* or not, via Cardano's formula [64]. The most general form of a cubic equation is given by

$$ax^3 + bx^2 + cx + d = 0, \quad (\text{D1})$$

where a, b, c, d are real.

The discriminant D is given by: $D = 18abcd - 4b^3d + b^2c^2 - 4ac^3 - 27a^2d^2$. Depending upon the sign of D , following three cases arise:

(a) $D < 0$, the cubic equation has two complex roots, so *casus irreducibilis* does not apply.

(b) $D = 0$, all three roots are real and expressible by real radicals.

(c) $D > 0$, there are three distinct real roots. In this case, a rational root exists and can be found using the rational root test. Otherwise, the given polynomial is *casus irreducibilis* and we need complex valued expressions to express the roots in radicals.

In our case, to solve Eq. (27), we have to solve the following cubic equation:

$$\gamma\omega_c^3 + 2\omega_h(\tau - \gamma)\omega_c^2 - \tau\omega_h^2(3 + \tau - \gamma)\omega_c + 2\tau^2\omega_h^3 = 0. \quad (\text{D2})$$

The discriminant D of the above equation is given by

$$\begin{aligned} D &= 4\omega_h^6(1 + \gamma)(1 + \tau)[3\gamma^2(3 - \tau) + \gamma^3 + 9\gamma\tau \\ &\quad + 3\gamma\tau^2 + 9\tau^2(1 - \tau)]. \end{aligned} \quad (\text{D3})$$

Since the parameters ω_h, γ, τ are positive and $\tau < 1, D > 0$. So the polynomial in Eq. (D2) presents the case of *casus irreducibilis*.

APPENDIX E: MAPPING TO FEYNMAN'S RATCHET AND PAWL MODEL

It is interesting to note that in the low-temperature regime, SSD refrigerator can be mapped to Feynman's ratchet and pawl model [65–69], a mesoscopic steady-state heat engine capable of extracting work from thermal fluctuations for a setup of two heat reservoirs via a ratchet and pawl mechanism. In the refrigerator mode, the ratchet makes a backward jump when x_c amount of heat is absorbed from the cold reservoir and subsequently x_h amount of heat is supplied to the hot reservoir [65,68]. Similarly, the wheel turns in the forward direction when x_h energy is absorbed from the hot reservoir. The rates of forward and backward jumps are given by

$$R_F = r_0 e^{-\hbar x_h/k_B T_h}, \quad R_B = r_0 e^{-\hbar x_c/k_B T_c}, \quad (E1)$$

where r_0 is the rate constant. The system operates as a refrigerator when $R_B > R_F$. The rates of heat exchanged with

the cold and hot reservoirs, respectively, are given by

$$\dot{Q}_c = x_c(R_B - R_F) = r_0 x_c (e^{-\hbar x_c/k_B T_c} - e^{-\hbar x_h/k_B T_h}), \quad (E2)$$

$$\dot{Q}_h = x_h(R_B - R_F) = r_0 x_h (e^{-\hbar x_c/k_B T_c} - e^{-\hbar x_h/k_B T_h}). \quad (E3)$$

Therefore, χ function for Feynman's model can be written as follows

$$\chi_F = \frac{r_0 x_c^2}{x_h - x_c} (e^{-\hbar x_c/k_B T_c} - e^{-\hbar x_h/k_B T_h}). \quad (E4)$$

Apart from the multiplicative constant $2\hbar\lambda^2\Gamma_c\Gamma_h/(\Gamma_c + \Gamma_h)(\lambda^2 + \Gamma_c\Gamma_h)$ (instead of r_0), the expression in Eq. (19) is similar to the χ function for the Feynman's model [Eq. (E4)], where ω_c and ω_h are replaced by x_c and x_h . Thus, we establish a mapping between our model of refrigerator and Feynman's model. A similar mapping also exists between the SSD engine and Feynman's ratchet as heat engine [36].

-
- [1] Z. Yan and J. Chen, *J. Phys. D: Appl. Phys.* **23**, 136 (1990).
 [2] D. C. Agrawal and V. J. Menon, *J. Phys. A* **23**, 5319 (1990).
 [3] A. E. Allahverdyan, K. Hovhannisyan, and G. Mahler, *Phys. Rev. E* **81**, 051129 (2010).
 [4] Y. Apertet, H. Ouerdane, A. Michot, C. Goupil, and P. Lecoeur, *Europhys. Lett.* **103**, 40001 (2013).
 [5] F. L. Curzon and B. Ahlborn, *Am. J. Phys.* **43**, 22 (1975).
 [6] M. Esposito, R. Kawai, K. Lindenberg, and C. Van den Broeck, *Phys. Rev. Lett.* **105**, 150603 (2010).
 [7] Y. Izumida and K. Okuda, *Europhys. Lett.* **97**, 10004 (2012).
 [8] I. Iyyappan and R. S. Johal, *Europhys. Lett.* **128**, 50004 (2020).
 [9] R. S. Johal, *Phys. Rev. E* **82**, 061113 (2010).
 [10] G. Thomas and R. S. Johal, *J. Phys. A* **48**, 335002 (2015).
 [11] R. S. Johal, *Europhys. Lett.* **121**, 50009 (2018).
 [12] R. S. Whitney, *Phys. Rev. Lett.* **112**, 130601 (2014).
 [13] R. S. Whitney, *Phys. Rev. B* **91**, 115425 (2015).
 [14] A. Ryabov and V. Holubec, *Phys. Rev. E* **93**, 050101(R) (2016).
 [15] V. Holubec and A. Ryabov, *J. Stat. Mech.* **07** (2016) 073204.
 [16] R. S. Johal, *Phys. Rev. E* **100**, 052101 (2019).
 [17] J. Guo, H. Yang, H. Zhang, J. Gonzalez-Ayala, J. Roco, A. Medina, and A. C. Hernández, *Energy Convers. Manag.* **198**, 111917 (2019).
 [18] C. de Tomás, A. C. Hernández, and J. M. M. Roco, *Phys. Rev. E* **85**, 010104(R) (2012).
 [19] Y. Izumida, K. Okuda, A. C. Hernández, and J. Roco, *Europhys. Lett.* **101**, 10005 (2013).
 [20] S. Velasco, J. M. M. Roco, A. Medina, and A. C. Hernández, *Phys. Rev. Lett.* **78**, 3241 (1997).
 [21] O. Abah and E. Lutz, *Europhys. Lett.* **113**, 60002 (2016).
 [22] L. A. Correa, J. P. Palao, G. Adesso, and D. Alonso, *Phys. Rev. E* **90**, 062124 (2014).
 [23] H. E. D. Scovil and E. O. Schulz-DuBois, *Phys. Rev. Lett.* **2**, 262 (1959).
 [24] J. Geusic, E. S.-D. Bois, R. De Grasse, and H. Scovil, *J. Appl. Phys.* **30**, 1113 (1959).
 [25] R. Kosloff, *Entropy* **15**, 2100 (2013).
 [26] G. Mahler, *Quantum Thermodynamic Processes: Energy and Information Flow at the Nanoscale* (Jenny Stanford Publishing, Singapore, 2014).
 [27] S. Vinjanampathy and J. Anders, *Contemp. Phys.* **57**, 545 (2016).
 [28] J. Millen and A. Xuereb, *New J. Phys.* **18**, 011002 (2016).
 [29] S. Deffner and S. Campbell, *Quantum Thermodynamics* (Morgan & Claypool Publishers, London, 2019).
 [30] R. Alicki and R. Kosloff, *Thermodynamics in the Quantum Regime* (Springer, Berlin, 2018), pp. 1–33.
 [31] *Thermodynamics in the Quantum Regime: Fundamental Aspects and New Directions*, edited by F. Binder, L. A. Correa, C. Gogolin, J. Anders, and G. Adesso (Springer, Berlin, 2018).
 [32] E. Geva and R. Kosloff, *Phys. Rev. E* **49**, 3903 (1994).
 [33] E. Geva and R. Kosloff, *J. Chem. Phys.* **104**, 7681 (1996).
 [34] R. Kosloff and A. Levy, *Annu. Rev. Phys. Chem.* **65**, 365 (2014).
 [35] K. E. Dorfman, D. Xu, and J. Cao, *Phys. Rev. E* **97**, 042120 (2018).
 [36] V. Singh and R. S. Johal, *Phys. Rev. E* **100**, 012138 (2019).
 [37] N. Jaseem, M. Hajdušek, V. Vedral, R. Fazio, L.-C. Kwek, and S. Vinjanampathy, *Phys. Rev. E* **101**, 020201(R) (2020).
 [38] J. Klatzow, J. N. Becker, P. M. Ledingham, C. Weinzetl, K. T. Kaczmarek, D. J. Saunders, J. Nunn, I. A. Walmsley, R. Uzdin, and E. Poem, *Phys. Rev. Lett.* **122**, 110601 (2019).
 [39] N. Linden, S. Popescu, and P. Skrzypczyk, *Phys. Rev. Lett.* **105**, 130401 (2010).
 [40] A. Levy and R. Kosloff, *Phys. Rev. Lett.* **108**, 070604 (2012).
 [41] L. A. Correa, J. P. Palao, G. Adesso, and D. Alonso, *Phys. Rev. E* **87**, 042131 (2013).
 [42] B. K. Agarwalla, J.-H. Jiang, and D. Segal, *Phys. Rev. B* **96**, 104304 (2017).
 [43] M. Kilgour and D. Segal, *Phys. Rev. E* **98**, 012117 (2018).
 [44] V. Holubec and T. Novotný, *J. Chem. Phys.* **151**, 044108 (2019).
 [45] G. Maslennikov, S. Ding, R. Hablützel, J. Gan, A. Roulet, S. Nimmrichter, J. Dai, V. Scarani, and D. Matsukevich, *Nat. Commun.* **10**, 202 (2019).
 [46] M. T. Mitchison, M. Huber, J. Prior, M. P. Woods, and M. B. Plenio, *Quant. Sci. Technol.* **1**, 015001 (2016).
 [47] J. B. Brask and N. Brunner, *Phys. Rev. E* **92**, 062101 (2015).

- [48] V. Gorini, A. Kossakowski, and E. C. G. Sudarshan, *J. Math. Phys.* **17**, 821 (1976).
- [49] G. Lindblad, *Commun. Math. Phys.* **48**, 119 (1976).
- [50] E. Boukobza and D. J. Tannor, *Phys. Rev. A* **74**, 063823 (2006).
- [51] E. Boukobza and D. J. Tannor, *Phys. Rev. A* **74**, 063822 (2006).
- [52] E. Boukobza and D. J. Tannor, *Phys. Rev. Lett.* **98**, 240601 (2007).
- [53] R. Alicki, *J. Phys. A* **12**, L103 (1979).
- [54] R. Kosloff, *J. Chem. Phys.* **80**, 1625 (1984).
- [55] E. Geva and R. Kosloff, *J. Chem. Phys.* **96**, 3054 (1992).
- [56] O. Abah, J. Roßnagel, G. Jacob, S. Deffner, F. Schmidt-Kaler, K. Singer, and E. Lutz, *Phys. Rev. Lett.* **109**, 203006 (2012).
- [57] L. A. Correa, J. P. Palao, D. Alonso, and G. Adesso, *Sci. Rep* **4**, 3949 (2014).
- [58] R. Uzdin and R. Kosloff, *Europhys. Lett.* **108**, 40001 (2014).
- [59] Y. Izumida, K. Okuda, J. M. M. Roco, and A. C. Hernández, *Phys. Rev. E* **91**, 052140 (2015).
- [60] Y. Yuan, R. Wang, J. He, Y. Ma, and J. Wang, *Phys. Rev. E* **90**, 052151 (2014).
- [61] Y. Wang, M. Li, Z. C. Tu, A. C. Hernández, and J. M. M. Roco, *Phys. Rev. E* **86**, 011127 (2012).
- [62] A. Mani and C. benjamin, *J. Phys. Chem. C* **123**, 22858 (2019).
- [63] I. Kleiner, *A History of Abstract Algebra* (Springer, Berlin, 2007), pp. 113–163.
- [64] I. Stewart, *Galois Theory* (Chapman and Hall/CRC, Boca Raton, FL, 1990).
- [65] R. P. Feynman, R. B. Leighton, and M. Sands, *The Feynman Lectures on Physics* (Narosa Publishing House, New Delhi, India, 2008).
- [66] J. M. R. Parrondo and P. Espanol, *Am. J. Phys.* **64**, 1125 (1996).
- [67] S.-Q. Sheng, P. Yang, and Z.-C. Tu, *Commun. Theor. Phys.* **62**, 589 (2014).
- [68] V. Singh and R. S. Johal, *Entropy* **19**, 576 (2017).
- [69] V. Singh and R. S. Johal, *J. Stat. Mech.* (2018) 073205.